

## **Title**

A 3D deep learning classifier and its explainability when assessing coronary artery disease

Wing Keung Cheung<sup>1</sup>, Jeremy Kalindjian<sup>2</sup>, Robert Bell<sup>2</sup>, Arjun Nair<sup>3</sup>, Leon J. Menezes<sup>4</sup>, Riyaz Patel<sup>5</sup>, Simon Wan<sup>4</sup>, Kacy Chou<sup>1</sup>, Jiahang Chen<sup>6</sup>, Ryo Torii<sup>6</sup>, Rhodri H. Davies<sup>5,7</sup>, James C. Moon<sup>7</sup>, Daniel C. Alexander<sup>1</sup>, Joseph Jacob<sup>1,8</sup>

<sup>1</sup>Satsuma Lab, Centre for Medical Image Computing & Department of Computer Science, University College London, London, UK

<sup>2</sup>Hatter Cardiovascular Institute, University College London, London, UK

<sup>3</sup>Department of Radiology, University College London Hospital, London, UK

<sup>4</sup>Institute of Nuclear Medicine, University College London, London, UK

<sup>5</sup>Institute of Cardiovascular Science, Faculty of Population Health Sciences, University College London, London, UK

<sup>6</sup>Department of Mechanical Engineering, University College London, London, UK

<sup>7</sup>Barts Heart Centre, West Smithfield, London, UK

<sup>8</sup>Department of Respiratory Medicine, University College London, London, UK

Corresponding author:

Dr Joseph Jacob

UCL Centre for Medical Image Computing

1st Floor, 90 High Holborn, London WC1V6LJ

[j.jacob@ucl.ac.uk](mailto:j.jacob@ucl.ac.uk)

## **Abstract**

Early detection and diagnosis of coronary artery disease (CAD) could save lives and reduce healthcare costs. In this study, we propose a 3D Resnet-50 deep learning model to directly classify normal subjects and CAD patients on computed tomography coronary angiography images. Our proposed method outperforms a 2D Resnet-50 model by 23.65%. Explainability is also provided by using a Grad-GAM. Furthermore, we link the 3D CAD classification to a 2D two-class semantic segmentation for improved explainability and accurate abnormality localisation.

## Introduction

Coronary artery disease (CAD) is a common cause of death [1] in developed (i.e., UK, USA) and developing countries (i.e., India, Philippines). Early detection and diagnosis of CAD could save lives and costs [2]. Currently, computed tomography coronary angiography (CTCA) plays a central role in diagnosing or excluding CAD in patients with chest pain [3, 4]. It has the ability to image stable and unstable atherosclerotic plaques which can result in coronary artery stenosis. The assessment of CAD severity is based on a clinicians' visual assessment of the severity of coronary artery narrowing on automated segmentation. This procedure, however, is subjective [5, 6] and the accuracy of the assessment is influenced by the experience of the clinician. Given the large number of suspected CAD patients in the NHS and the existing shortage of clinicians available to review the CTCA [7], it is crucial to develop fast, efficient, objective and accurate automated detection and classification systems to assist clinicians to diagnose CAD. This will also enable faster triage of patients using computer technology on local hospital servers, speeding up diagnosis and patient management.

Deep learning [8] is a promising method to deliver fully automatic diagnosis for CAD. It utilises image data and GPU technology to provide fast and efficient computation. Deep learning based CAD diagnosis on CTCA can be broadly divided into two categories, (1) CAD segmentation [9] (2) CAD classification [10]. CAD segmentation aims to produce a segmented mask containing the proximal ascending aorta and the coronary arteries. The mask is particularly useful for visual estimation of stenosis severity. Further, it can be used for computational fluid dynamics (CFD) [11] which can estimate the blood flow in the coronary vessels. This clinical information is important for diagnosing hemodynamically significant CAD. On the other hand, CAD classification aims to grade CAD severity (i.e., no CAD, non-obstructive CAD and obstructive (severe) CAD) [12]. This can be achieved by predicting a severity label at the patient-level. A deep learning based classifier may use CTCA images and learn the non-linear mapping between image features and CAD severity grades. It offers robust and efficient classification and can be implemented easily on local hospital servers.

Deep learning methods have been implemented successfully for medical image segmentation and classification. However, one of the drawbacks of deep learning is that its black box nature limits its interpretability and therefore clinical applicability as end users may struggle to understand the decisions of the classifier. Therefore, the deep learning research community has increasingly focused on explainability. Explainable AI (XAI) [13] aims to provide explainable tools for deep learning methods. This can improve confidence and trust for end users in deep learning output. In the context of CTCA image classification, a popular XAI tools is Grad-GAM [14]. It allows direct visualisation of regions in the image that the deep learning model found to be important. The Grad-CAM employs gradient-weighted class activation mapping and provides visual explanations for deep learning based classifiers.

Previous studies related to deep learning based CAD segmentation are summarised in [15]. More recently, Lin et al. [16] have proposed the hierarchical convolutional long short-term memory (ConvLSTM) network to segment the coronary arteries. It demonstrated excellent

agreement between deep learning and expert readers for volumes of total plaque, calcified plaque and non-calcified plaque. Song et al. [17] have developed a three-stage approach to segment the coronary arteries. A 2D DenseNet was first employed to classify coronary arteries and non-coronary arteries. Then, a 3D FFR-Unet was used to segment the initial coronary arteries. The final segmentation results were obtained by performing Gaussian weighted averaging on the segmentation predictions.

The studies related to deep learning based CAD classification are summarised in this review [10]. Furthermore, Raghav et al. [18] demonstrated an automated CNN model based on a Shufflenet architecture for detecting CAD from CTCA with high accuracy. The drawback of this approach is that it requires slice-level annotations, which are time consuming and labour intensive. Further, the model is not able to localise the abnormality in the coronary artery. Zreik et al. [19] proposed a 3D recurrent CNN for automatic detection and classification of coronary artery plaque and stenosis in coronary CT angiography. The drawback of this method is that it requires extraction of a centerline and the 3D CNN model requires high GPU memory. Candemir et al. [20] developed a 3D CNN deep learning model to classify the coronary arteries and localise abnormal regions. It also requires centerline extraction and high GPU memory. The above approaches reduce the computational and GPU memory efficiency.

The studies related to explainability of deep learning based CAD classification are limited. Salih et al. [21] reviewed XAI methods in cardiac imaging. Though the study considered cardiac magnetic resonance (CMR) imaging, the XAI techniques are applicable to CTCA. Candemir et al. [20] used a weakly supervised method to localise coronary abnormalities, thereby confirming that the 3D CNN model focused on stable and unstable plaques. However, abnormality localisation was still not exact.

Currently, no studies focus on direct and explainable approaches for CAD classification. In this study, we propose a 3D deep learning approach with explainability for the automated classification of normal subjects and CAD patients on CTCA images.

The main contributions of this study are:

- The first study to propose a 3D Resnet-50 deep learning model that directly classifies normal subjects and patients with coronary artery disease on CTCA images.
- Compared with a 2D Resnet-50, our proposed method provides a better classification accuracy by 23.65%.
- Our proposed method is fast, efficient and particularly good at classifying normal subjects on CTCA images and requires only subject-level labels.

- Explainability is reported though it does not focus on the coronary arteries. We suggest informed cues could be used to improve the explainability.
- The study links the 3D CAD classification to 2D two-class semantic segmentation, and the semantic segmentation provides better explainability and accurate abnormality localisation.

## Methods

### *Patient data*

The data were collected from University College Hospital London and Barts Health NHS Trust. CTCA scans were performed on 88 subjects. All the patients in the study had been evaluated for possible angina, with an intermediate risk of coronary artery disease. All patients underwent cardiac CT angiography for anatomical assessment of their coronary arteries and risk stratification for coronary artery disease. The study was carried out in accordance with the recommendations of the South East Research Ethics Committee, Aylesford, Kent, UK, and Leeds East Research Ethics Committee: 20/YH/0120 with written informed consent from all subjects in accordance with the Declaration of Helsinki.

### *Data pre-processing*

The CTCA images were pre-processed using ImageJ (1.53). The intensity of the images were normalised using linear histogram stretch and subsequently rescaled to between 0 to 255. The images were resized from 512x512 to 128x128. The processed images were saved to 8-bit Portable Network Graphics (PNG). The images were used to feed the deep learning models for training, validation and testing. It should be noted that the total number of slices (per case) was resampled to 256 for 3D CAD classification.

### *Data annotation*

An experienced cardiologist performed the data annotation. The labels were produced at subject level. When abnormal features (i.e., calcification, stenosis) were observed in subjects' CT volumetric images, CAD (abnormal) labels were assigned to the subjects' CT images. Otherwise, normal labels were assigned.

### *2D CAD classification*

The 2D Resnet-50 was used to perform 2D CAD classification. It is a 50-layer convolutional network and utilises shortcut connections to form a residual network. Shortcut connections improve the information and gradients to flow more easily throughout the network. The network adopts a bottleneck design strategy, which has 1x1 convolutions. This reduces the number of parameters and matrix multiplications and therefore allows faster training on each layer. Figure 1 shows the network architecture of 2D Resnet-50.

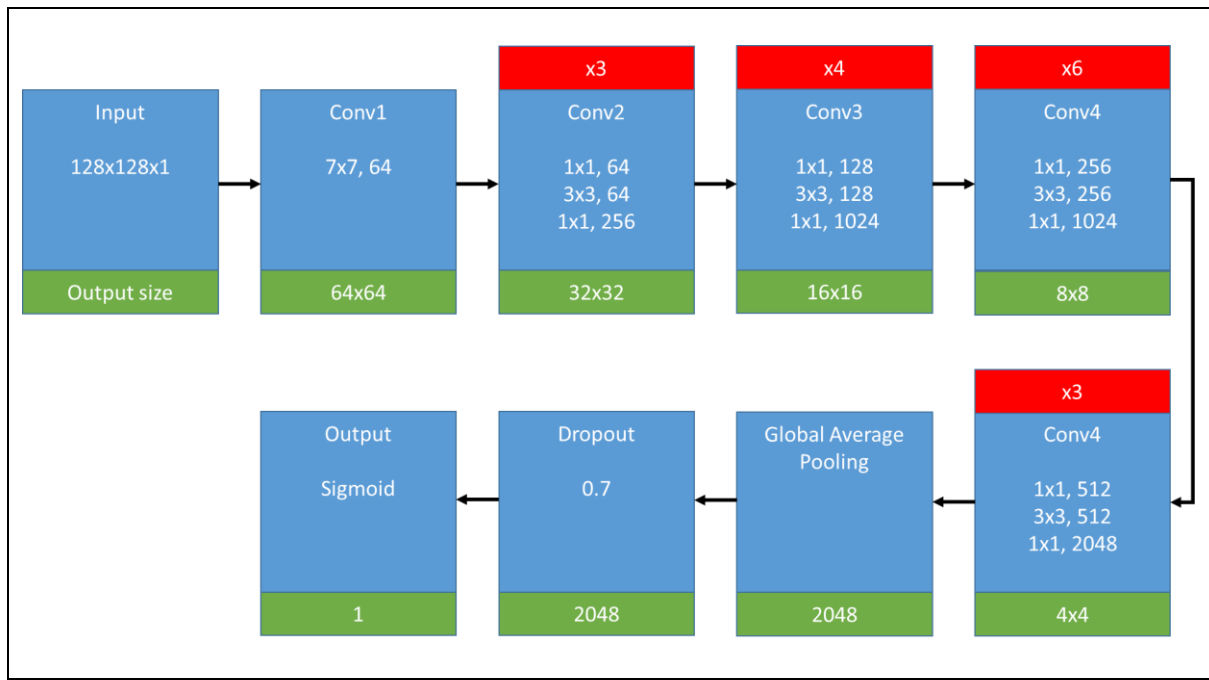


Figure 1: 2D Resnet-50 architecture.

### 3D CAD classification

3D CAD classification was performed using 3D Resnet-50. The 3D Resnet-50 network is the extension of the 2D Resnet-50 network. It uses 1x1x1 convolutions for bottleneck block. It has the ability to learn features across several images while the 2D Resnet-50 learns the features within a single image only. The network architecture of 3D Resnet-50 is shown in Figure 2.

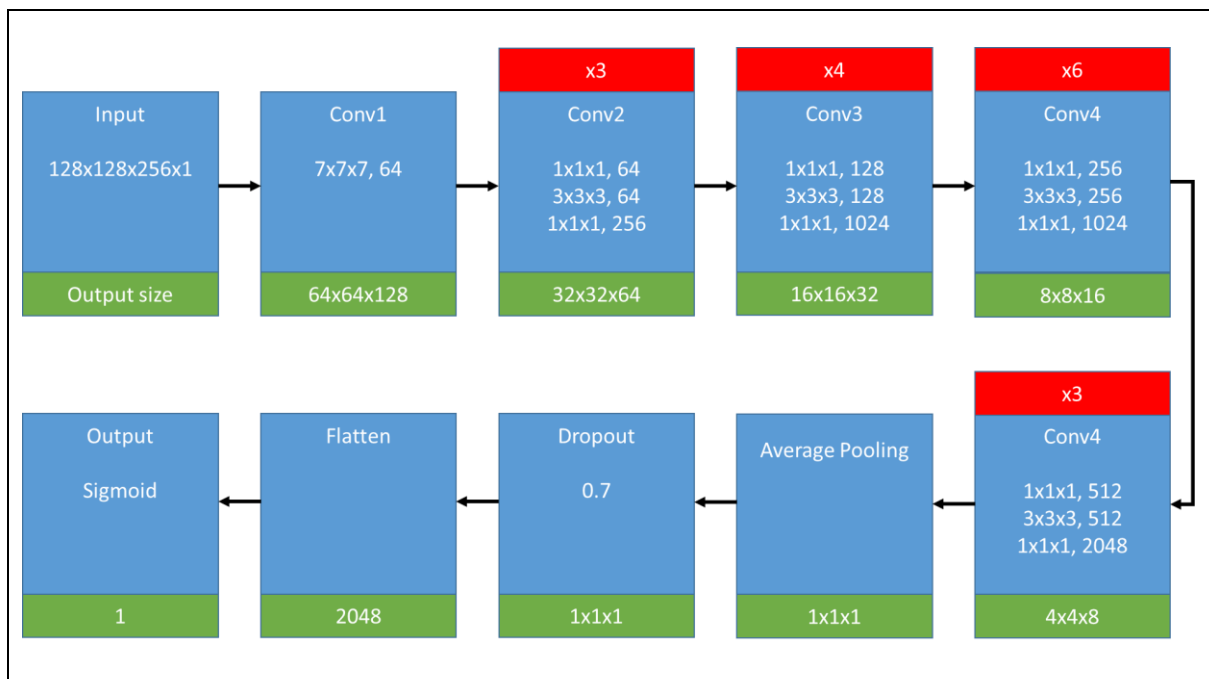


Figure 2: 3D Resnet-50 architecture.

### 2D two-class semantic segmentation

The link between 3D CAD classification and 2D two-class semantic segmentation was demonstrated in this study. 3D CAD classification was treated as a 2D two-class (aorta and coronary arteries vs non-aorta and non-coronary arteries) semantic segmentation. The segmentation of aorta and coronary arteries and its explainability were done in our previous studies [15, 22]. A 2D modified U-Net was employed to segment the target tissues, Furthermore, the explainability of the proposed method was investigated. Firstly, the 2D binary segmentation was converted to a 2D two-class semantic segmentation. Then, the trained model was analysed by Seg-Grad-CAM [23]. The Seg-Grad-CAM employs gradient-weighted class activation mapping and provides a method for explaining the segmentation decision.

### Model training and implementation

The clinical data was split into training, validation and test sets. The ratio of normal subjects to CAD patients was maintained for each set. Table 1 shows the number of normal subjects and CAD patients in each set. Moreover, the corresponding total slices for each set is summarised in Table 2. It should be noted that 3D classification is performed at a subject level, while 2D classification is performed at a CT slice level.

Table 1: Cases allocation for training, validation and test sets.

<b>Cases</b>	<b>Normal subject</b>	<b>CAD patient</b>	<b>Total</b>
<i>Training set</i>	30	30	60
<i>Validation set</i>	7	7	14
<i>Test set</i>	7	7	14
<b>Total</b>	44	44	88

Table 2: Slices allocation for training, validation and test sets.

<b>Slices</b>	<b>Normal subject</b>	<b>CAD patient</b>	<b>Total</b>
<i>Training set</i>	8173	7762	15935
<i>Validation set</i>	2200	2014	4214
<i>Test set</i>	1946	2153	4099
<b>Total</b>	12319	11929	24248

The proposed Resnet-50 models were implemented in Tensorflow (2.12.0). They were executed on two high performance machines with the following configurations: (1) Intel Xeon CPU @2.20 GHz with a Nvidia Tesla K80 accelerator (2) AMD EPYC 7313 @3.00 GHz 16-Core Processor with a Nvidia RTX A6000. The optimal weights and biases were computed by using Adam optimiser. When the training did not improve after three epochs, the learning rate (initial learning rate =  $1e^{-3}$ ) was subsequently reduced by a factor of 0.1. Early stopping was implemented when the training was not improved after 10 consecutive epochs.

### *Loss function and performance evaluation*

In this study, binary cross entropy (BCE) was employed for training the deep learning models. It is commonly used for binary classification. Furthermore, accuracy, recall, precision and F1-score were used to measure the classification performance.

### *Classification Explainability*

The explainability of the proposed methods was investigated by Grad-CAM [14]. The first, middle and last convolution layers from the proposed models were selected for this study. The Grad-CAM produces a heat map and highlights the regions in the image which are important for the classification.

## **Results**

### *Classification accuracy*

Table 3 shows the classification accuracy of 2D and 3D Resnet-50 models. The 2D Resnet-50 achieved 97.80%, 52.23% and 47.78% for training, validation and test accuracies respectively. The proposed model (3D Resnet-50) achieved 61.67%, 71.43% and 71.43% for training, validation and test accuracies respectively. Our proposed model outperformed the 2D Resnet-50 model by 23.65% on test accuracy.

Table 3: The classification accuracy of 2D and 3D Resnet-50 models.

<b>Classification model</b>	<b>Training Accuracy</b>	<b>Validation Accuracy</b>	<b>Test Accuracy</b>
2D Resnet-50	97.80%	52.23%	47.78%
3D Resnet-50	61.67%	71.43%	71.43%

With regard to recall, precision and F1-score measurements, our proposed model outperformed the 2D Resnet-50 model on both validation and test sets. On the validation set, our approach achieved 0.71, 0.71 and 0.71 for recall, precision and F1-score respectively. The 2D Resnet-50 model achieved 0.06, 0.48 and 0.11 for recall, precision and F1-score respectively. On the test set, our approach achieved 0.43, 1.00 and 0.60 for recall, precision and F1-score respectively. The 2D Resnet-50 model achieved 0.06, 0.52 and 0.11 for recall, precision and F1-score respectively. The recall, precision and F1-score of 2D and 3D Resnet-50 models for validation and test sets are shown in Table 4.

Table 4: The recall, precision and F1-score of 2D and 3D Resnet-50 models for validation and test sets.

<b>Classification model</b>	<b>Recall</b>		<b>Precision</b>		<b>F1-score</b>	
	<i>Validation</i>	<i>Test</i>	<i>Validation</i>	<i>Test</i>	<i>Validation</i>	<i>Test</i>
2D Resnet-50	0.06	0.06	0.48	0.52	0.11	0.11
3D Resnet-50	0.71	0.43	0.71	1.00	0.71	0.60

### Confusion matrix for validation and test sets

Tables 5 and 6 show the true positive (TP), false positive (FP), false negative (FN) and true negative (TN) measurements for 2D and 3D Resnet-50 models. On the validation set, 2D Resnet-50 model produced 2.99%, 3.35%, 44.80% and 48.01% for TP, FP, FN and TN respectively, while our proposed model produced 35.71%, 14.29%, 14.29% and 35.71% for TP, FP, FN and TN respectively. On test set, 2D Resnet-50 model produced 3.24%, 3.00%, 49.28% and 44.47% for TP, FP, FN and TN respectively, while our proposed model produced 21.43%, 0.00%, 28.57% and 50.00% for TP, FP, FN and TN respectively. Our proposed model performed better than 2D Resnet-50 model by 18.19%, 3.00%, 20.71% and 5.53% for TP, FP, FN and TN respectively on test set.

Table 5: The TP, FP, FN and TN measurements for 2D Resnet-50 model.

	<b>TP</b>	<b>FP</b>	<b>FN</b>	<b>TN</b>
Validation set (4214 slices)	126 (2.99%)	137 (3.25%)	1888 (44.80%)	2063 (48.01%)
Test set (4099 slices)	133 (3.24%)	123 (3.00%)	2020 (49.28%)	1823 (44.47%)

Table 6: The TP, FP, FN and TN measurements for 3D Resnet-50 model.

	<b>TP</b>	<b>FP</b>	<b>FN</b>	<b>TN</b>
Validation set (14 cases)	5 (35.71%)	2 (14.29%)	2 (14.29%)	5 (35.71%)
Test set (14 cases)	3 (21.43%)	0 (0.00%)	4 (28.57%)	7 (50.00%)

### Explainability

One normal subject and one CAD patient with a correct prediction were selected to illustrate the explainability. Corresponding normal and abnormal slices were chosen accordingly. Figure 3 shows the Grad-GAM generated by 2D Resnet-50 from last, middle and first convolution layers on a normal subject and a CAD patient respectively. Figure 4 shows the Grad-GAM generated by 3D Resnet-50 from last, middle and first convolution layers on a normal subject and a CAD patient respectively.

#### (1) 2D CAD classification by 2D Resnet-50 model

On the last convolution layer, the model focused on the region around the spinal cord for both the normal subject and CAD patient. On the middle convolution layer, the model focused on the right lung for the normal subject while the model focused on the central region including left lung, right lung and heart for the CAD patient. On the first convolution layer, the model did not capture important features for both normal subjects and CAD patients.

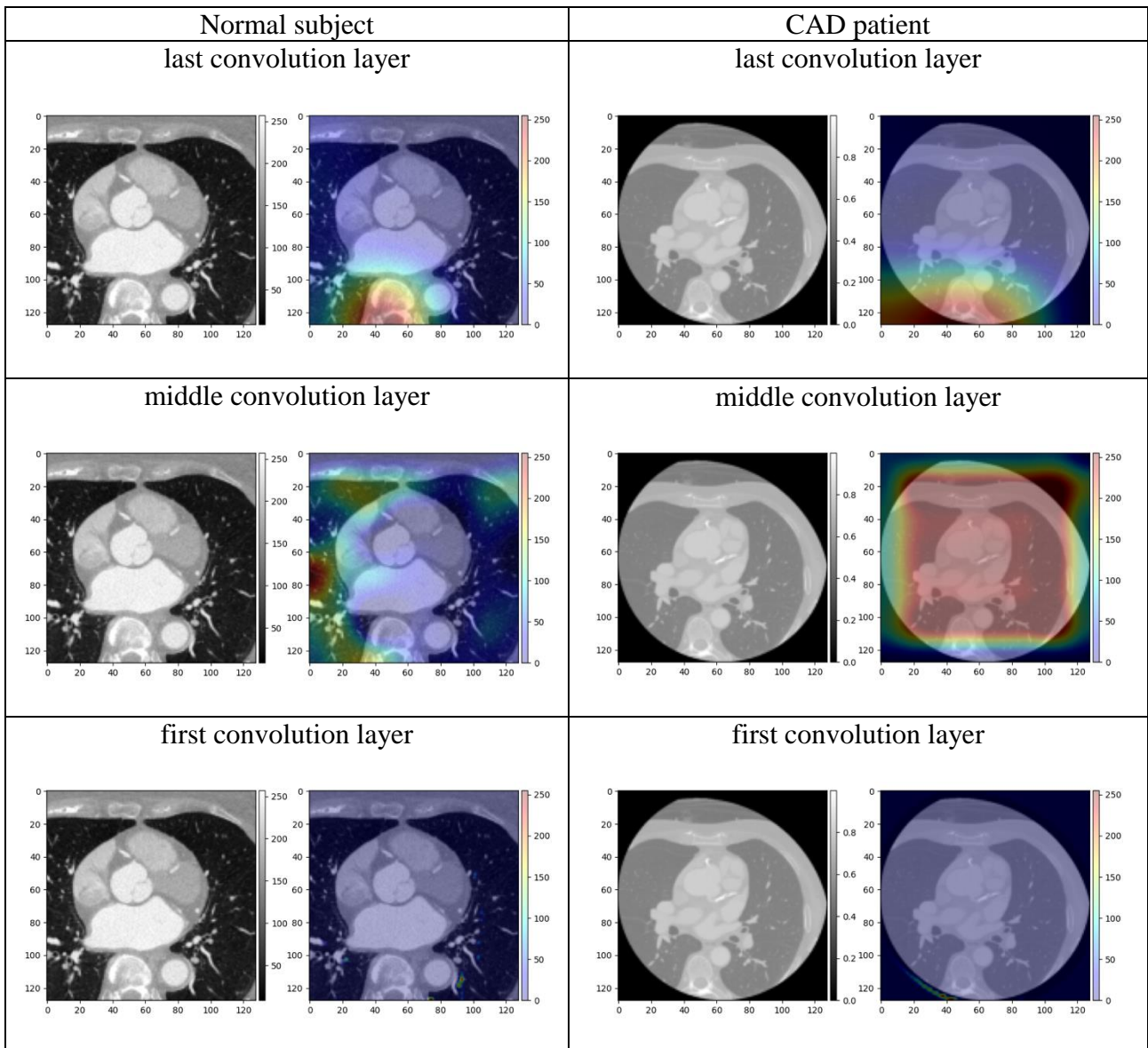


Figure 3: The Grad-GAM generated by 2D Resnet-50 from last, middle and first convolution layers on a normal subject and a CAD patient.

## (2) 3D CAD classification by 3D Resnet-50 model

On the last convolution layer, the model focused on the region around the spinal cord and descending aorta for the normal subject, while the model focused on the far left lung for the CAD patient. On the middle convolution layer, the model focused on the region around the spinal cord and descending aorta for the normal subject, while the model focused on the right lung for the CAD patient. On the first convolution layer, the model did not capture important features for the normal subject, while the model focused on the background for the CAD patient.

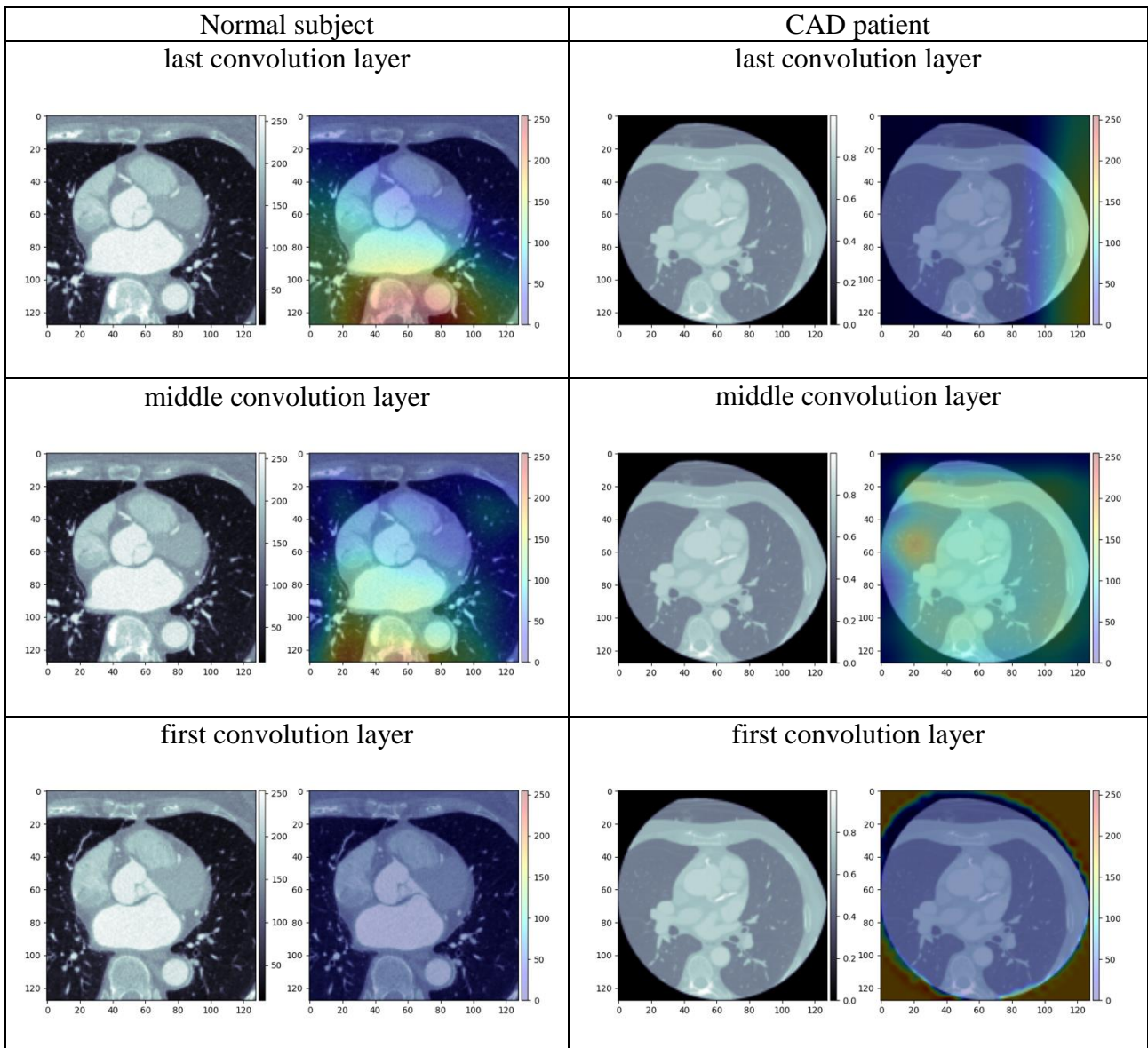


Figure 4: The Grad-GAM generated by 3D Resnet-50 from last, middle and first convolution layers on a normal subject and a CAD patient.

### (3) 2D two-class semantic segmentation by 2D modified U-Net model

Figures 5 and 6 shows the aorta and coronary arteries segmentation and its explainability. It confirms that the deep learning model focused on the aorta and coronary arteries for the segmentation task. Further, the modified U-Net showed a good segmentation performance (DSC = 91.2%). We observed that a 2D deep learning based semantic (two-class) segmentation provides a better solution for accurate classification and explainability with exact abnormality localisation.

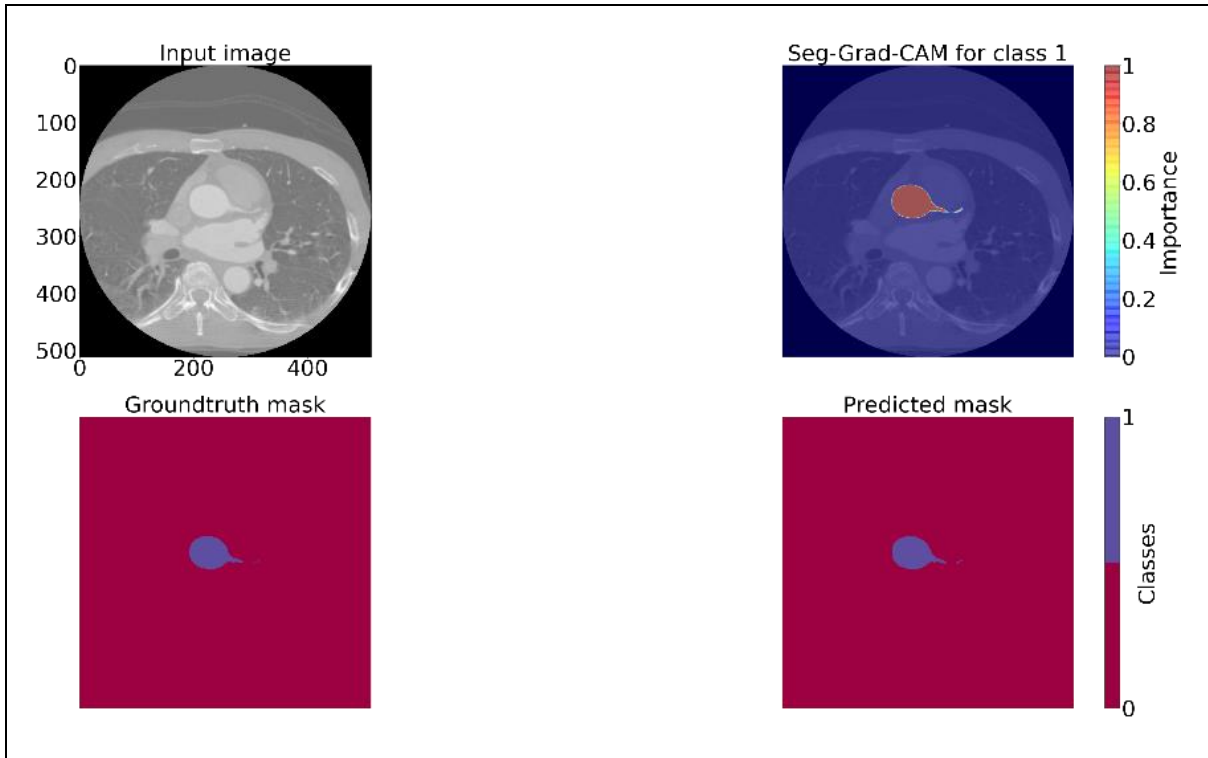


Figure 5: An example of selected CTCA slice and its ground-truth mask, Seg-Grad-CAM for aorta and coronary arteries and predicted mask. Part of the image is reproduced with permission from [22].

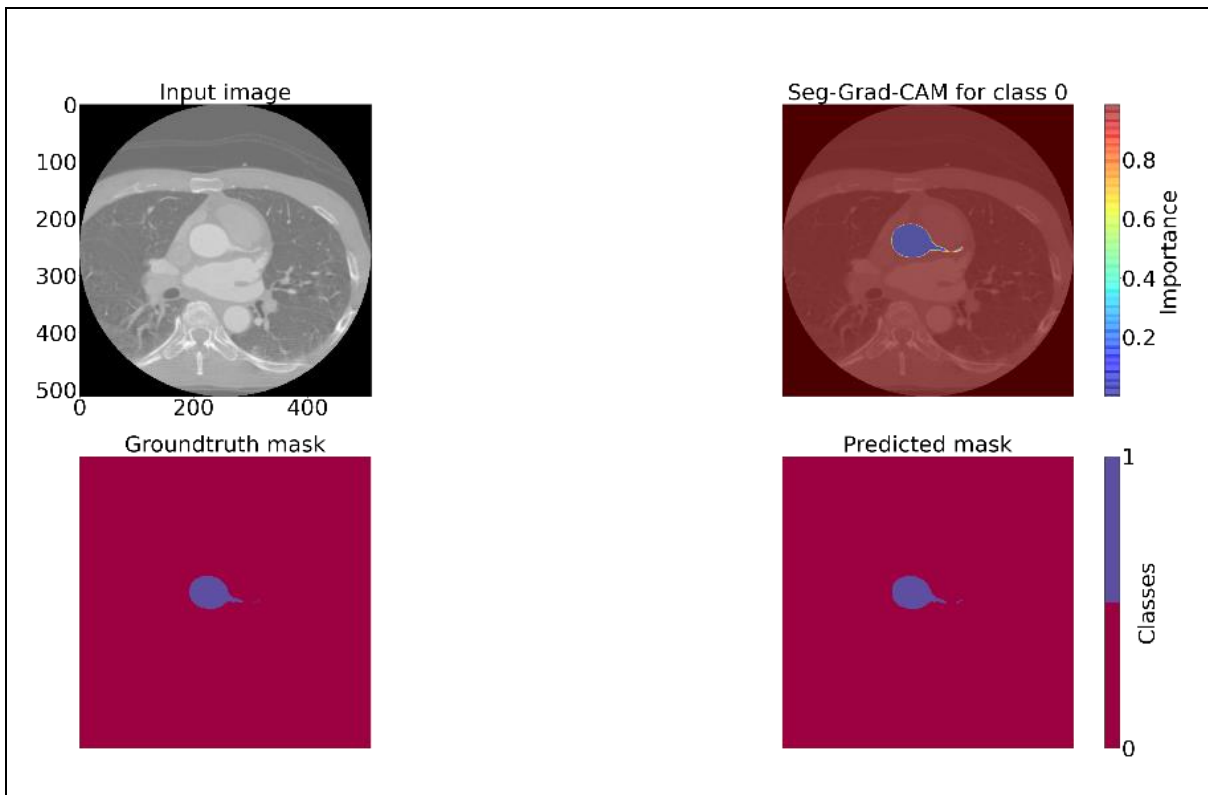


Figure 6: An example of selected CTCA slice and its ground-truth mask, Seg-Grad-CAM for non-aorta and non-coronary arteries and predicted mask. Part of the image is reproduced with permission from [22].

## Discussion

A 3D deep learning based classifier has been proposed to classify CAD patients from CTCA images. It adopts a 3D Resnet-50 model to classify normal subjects and patients with CAD. Its classification accuracy is better than a 2D Resnet-50 by 23.65%. Our proposed model has excellent precision and fair recall, which implies that it does not misclassify normal subjects as CAD patients and can identify normal subjects.

In this study, we observe that overfitting of a 2D Resnet-50 model can lead to poor classification performance. The overfitting is due to memorisation of inaccurate labels. The classification performance could be improved by introducing an automatic inaccurate label correction method [24]. It should be noted that our previous study [25] produced better classification accuracy than the current study as it employed unbalanced datasets for training, validation and test. Therefore, the previous results were biased towards CAD cases. Our current study employed balanced datasets for all sets, and therefore produced unbiased results for both normal and CAD cases.

Explainability has also been reported in this study. In terms of abnormality localisation, Grad-CAM does not produce a focused heat map on the last convolution layer for our proposed model. A relatively focused heat map can be observed on the middle convolution layer. Compared with 2D Resnet-50 model, a better heat map can be observed on the middle convolution layer, but it is less focused than our proposed model.

Recently, Ghassemi et al. [26] have discussed the inaccuracy of the heat map. Given that the annotation is at patient-level, the generated heat map does not highlight the abnormality exactly, limiting interpretability for clinicians. Based on our observations in this study, we deduce that deep learning models do not require exact abnormality localisation in order to perform accurate classification. Further, the accuracy/usefulness of the explainability depends on the level of annotation (i.e., annotation at patient level vs annotation at pixel/voxel level). An alternative way to increase the annotation level is to incorporate prior information into the deep learning model (i.e., informed cue [27]). In the context of CAD classification, these cues could be either (1) centreline extraction along the aorta and coronary arteries or (2) a mask containing the aorta and coronary arteries. These cues could help a deep learning model focus on important regions known to clinicians. The associated heat map could provide better explainability thereby meeting clinicians' expectations.

We demonstrate the reasoning above by treating 3D CAD classification as a 2D two-class (aorta and coronary arteries vs non-aorta and non-coronary arteries) semantic segmentation. It confirms that the deep learning model focused on the aorta and coronary arteries for the segmentation task. We conclude that a 2D deep learning based semantic (two-class)

segmentation provides a better solution for accurate classification and explainability with exact abnormality localisation.

In practice, we suggest that the design of a deep learning method and its explainability should meet the clinicians' requirements for explainability. This could improve the trust and transparency of a deep learning model and make it easier to be deployed in the clinical setting.

The study has several limitations. First, the study is retrospective, the selection of patients might be biased. Second, the slice thickness might limit the visibility of very small coronary arteries on CTCA images. Lastly, the relatively small dataset might limit the generalisation of the proposed deep learning model.

In future work we hope to incorporate the mask of the aorta and coronary arteries into 3D CAD classification and further improve classification accuracy and explainability. The 2D 2-class semantic segmentation can be extended to 3D multi-class (i.e., aorta and coronary arteries, stable plaques and unstable plaques) segmentation, for more accurate classification and explainability with exact abnormality localisation.

## **Conclusion**

A 3D deep learning based CAD classifier has been proposed and the associated explainability has been reported. The link between CAD classification and segmentation is discussed. Suggestions are made to further improve the classification accuracy and explainability.

## **Acknowledgement**

The authors acknowledge Mr Xiaoxia Yang for his assistance with data processing for aorta and coronary artery segmentation. JJ was supported by Wellcome Trust Clinical Research Career Development Fellowship 209553/Z/17/Z and the NIHR Biomedical Research Centre at University College London. This research was funded in whole or in part by the Wellcome Trust [209553/Z/17/Z]. For the purpose of open access, the author has applied a CC-BY public copyright licence to any author accepted manuscript version arising from this submission.

## **Declaration of Interest**

JJ declares fees from Boehringer Ingelheim, F. Hoffmann-La Roche, GlaxoSmithKline, NHSX, Takeda, Wellcome Trust, Microsoft Research unrelated to the submitted work and UK patent application numbers 2113765.8 and GB2211487.0.

## References

- [1] H. Wang *et al.*, "Global, regional, and national life expectancy, all-cause mortality, and cause-specific mortality for 249 causes of death, 1980–2015: a systematic analysis for the Global Burden of Disease Study 2015," *The Lancet*, vol. 388, no. 10053, pp. 1459-1544, 2016/10/08/ 2016, doi: [https://doi.org/10.1016/S0140-6736\(16\)31012-1](https://doi.org/10.1016/S0140-6736(16)31012-1).
- [2] M. J. Bom *et al.*, "Early Detection and Treatment of the Vulnerable Coronary Plaque: Can We Prevent Acute Coronary Syndromes?," (in English), *Circ-Cardiovasc Imag*, vol. 10, no. 5, May 2017, doi: 10.1161/CIRCIMAGING.116.005973.
- [3] P. I. Ngam, C. C. Ong, P. Chai, S. S. Wong, C. R. Liang, and L. L. S. Teo, "Computed tomography coronary angiography - past, present and future," (in eng), *Singapore Med J*, vol. 61, no. 3, pp. 109-115, 2020, doi: 10.11622/smedj.2020028.
- [4] "National Institute for Health and Care Excellence (NICE). Recent-onset chest pain of suspected cardiac origin: assessment and diagnosis Clinical guideline [CG95] <https://www.nice.org.uk/guidance/cg95>," 2016.
- [5] S. C. Saur *et al.*, "Effect of reader experience on variability, evaluation time and accuracy of coronary plaque detection with computed tomography coronary angiography," (in English), *Eur Radiol*, vol. 20, no. 7, pp. 1599-1606, Jul 2010, doi: 10.1007/s00330-009-1709-7.
- [6] F. Pugliese *et al.*, "Learning Curve for Coronary CT Angiography: What Constitutes Sufficient Training?," (in English), *Radiology*, vol. 251, no. 2, pp. 359-368, May 2009, doi: 10.1148/radiol.2512080384.
- [7] "Radiology workforce census 2020." [Online]. Available: <https://www.rcr.ac.uk/press-and-policy/policy-priorities/workforce/radiology-workforce-census>.
- [8] Y. LeCun, Y. Bengio, and G. Hinton, "Deep learning," *Nature*, vol. 521, no. 7553, pp. 436-444, 2015/05/01 2015, doi: 10.1038/nature14539.
- [9] C. Chen *et al.*, "Deep Learning for Cardiac Image Segmentation: A Review," *Front Cardiovasc Med*, vol. 7, p. 25, 2020, doi: 10.3389/fcvm.2020.00025.
- [10] N. Hampe, J. M. Wolterink, S. G. M. van Velzen, T. Leiner, and I. Isgum, "Machine Learning for Assessment of Coronary Artery Disease in Cardiac CT: A Survey," *Front Cardiovasc Med*, vol. 6, p. 172, 2019, doi: 10.3389/fcvm.2019.00172.
- [11] Z. Sun and L. Xu, "Computational fluid dynamics in coronary artery disease," *Computerized Medical Imaging and Graphics*, vol. 38, no. 8, pp. 651-663, 2014/12/01/ 2014, doi: <https://doi.org/10.1016/j.compmedimag.2014.09.002>.
- [12] S. S. Zghebi *et al.*, "Assessing the severity of cardiovascular disease in 213 088 patients with coronary heart disease: a retrospective cohort study," *Open Heart*, vol. 8, no. 1, Apr 2021, doi: 10.1136/openhrt-2020-001498.
- [13] G. Vilone and L. Longo, "Explainable artificial intelligence: a systematic review," *arXiv preprint arXiv:2006.00093*, 2020.
- [14] R. R. Selvaraju, M. Cogswell, A. Das, R. Vedantam, D. Parikh, and D. Batra, "Grad-CAM: Visual Explanations from Deep Networks via Gradient-Based Localization," (in English), *Int J Comput Vision*, vol. 128, no. 2, pp. 336-359, Feb 2020, doi: 10.1007/s11263-019-01228-7.
- [15] W. K. Cheung *et al.*, "A Computationally Efficient Approach to Segmentation of the Aorta and Coronary Arteries Using Deep Learning," *IEEE Access*, vol. 9, pp. 108873-108888, 2021, doi: 10.1109/ACCESS.2021.3099030.
- [16] A. Lin *et al.*, "Deep learning-enabled coronary CT angiography for plaque and stenosis quantification and cardiac risk prediction: an international multicentre study,"

- Lancet Digit Health*, vol. 4, no. 4, pp. e256-e265, Apr 2022, doi: 10.1016/S2589-7500(22)00022-X.
- [17] A. Song *et al.*, "Automatic Coronary Artery Segmentation of CCTA Images With an Efficient Feature-Fusion-and-Rectification 3D-UNet," *IEEE J Biomed Health Inform*, vol. 26, no. 8, pp. 4044-4055, Aug 2022, doi: 10.1109/JBHI.2022.3169425.
- [18] P. Raghav, S. Rathore, S. Jain, S. Kumar, R. Madhok, and S. Rathore, "TCT CONNECT-192 Automated Classification of Computed Tomography Coronary Angiogram as Normal and Abnormal Using High-Sensitivity Deep-Learning Algorithm," *Journal of the American College of Cardiology*, vol. 76, no. 17 Supplement S, pp. B82-B82, 2020, doi: doi:10.1016/j.jacc.2020.09.205.
- [19] M. Zreik, R. W. v. Hamersvelt, J. M. Wolterink, T. Leiner, M. A. Viergever, and I. Išgum, "A Recurrent CNN for Automatic Detection and Classification of Coronary Artery Plaque and Stenosis in Coronary CT Angiography," *IEEE Transactions on Medical Imaging*, vol. 38, no. 7, pp. 1588-1598, 2019, doi: 10.1109/TMI.2018.2883807.
- [20] S. Candemir *et al.*, "Automated coronary artery atherosclerosis detection and weakly supervised localization on coronary CT angiography with a deep 3-dimensional convolutional neural network," *Computerized Medical Imaging and Graphics*, vol. 83, p. 101721, 2020/07/01/ 2020, doi: <https://doi.org/10.1016/j.compmedimag.2020.101721>.
- [21] A. Salih *et al.*, "Explainable Artificial Intelligence and Cardiac Imaging: Toward More Interpretable Models," *Circ Cardiovasc Imaging*, vol. 16, no. 4, p. e014519, Apr 2023, doi: 10.1161/CIRCIMAGING.122.014519.
- [22] W. K. Cheung, "State-of-the-art deep learning method and its explainability for computerized tomography image segmentation," *Explainable AI in healthcare: Unboxing machine learning for biomedicine*, M. S. Raval, M. Roy, T. Kaya, and R. Kapdi, Eds.: Chapman and Hall/CRC, 2023. [Online]. Available: <https://doi.org/10.1201/9781003333425-5>
- [23] K. Vinogradova, A. Dibrov, and G. Myers, "Towards Interpretable Semantic Segmentation via Gradient-Weighted Class Activation Mapping," (in English), *Aaai Conf Artif Inte*, vol. 34, pp. 13943-13944, 2020. [Online]. Available: <Go to ISI>://WOS:000668126806164.
- [24] S.-Y. Li, Y. Shi, S.-J. Huang, and S. Chen, "Improving deep label noise learning with dual active label correction," *Machine Learning*, vol. 111, no. 3, pp. 1103-1124, 2022/03/01 2022, doi: 10.1007/s10994-021-06081-9.
- [25] K. Chou, "2D Convolutional Neural Networks for Computer-Aided Detection in Cardiac Radiology," *Thesis, MSc in Business Analytics (with specialisation in Computer Science)*, UCL School of Management, University College London, 2019.
- [26] M. Ghassemi, L. Oakden-Rayner, and A. L. Beam, "The false hope of current approaches to explainable artificial intelligence in health care," *Lancet Digit Health*, vol. 3, no. 11, pp. e745-e750, Nov 2021, doi: 10.1016/S2589-7500(21)00208-9.
- [27] L. v. Rueden *et al.*, "Informed Machine Learning – A Taxonomy and Survey of Integrating Prior Knowledge into Learning Systems," *IEEE Transactions on Knowledge and Data Engineering*, vol. 35, no. 1, pp. 614-633, 2023, doi: 10.1109/TKDE.2021.3079836.